

ChemComm

Accepted Manuscript



This is an *Accepted Manuscript*, which has been through the Royal Society of Chemistry peer review process and has been accepted for publication.

Accepted Manuscripts are published online shortly after acceptance, before technical editing, formatting and proof reading. Using this free service, authors can make their results available to the community, in citable form, before we publish the edited article. We will replace this *Accepted Manuscript* with the edited and formatted *Advance Article* as soon as it is available.

You can find more information about *Accepted Manuscripts* in the [Information for Authors](#).

Please note that technical editing may introduce minor changes to the text and/or graphics, which may alter content. The journal's standard [Terms & Conditions](#) and the [Ethical guidelines](#) still apply. In no event shall the Royal Society of Chemistry be held responsible for any errors or omissions in this *Accepted Manuscript* or any consequences arising from the use of any information it contains.



Journal Name

COMMUNICATION

“Half-Sandwich” Yb^{III} Single-Ion Magnets with Metallacrown†

Quan-Wen Li, Jun-Liang Liu, Jian-Hua Jia,* Yan-Cong Chen, Jiang Liu, Long-Fei Wang and Ming-Liang Tong*

Received 00th January 20xx,
Accepted 00th January 20xx

DOI: 10.1039/x0xx00000x

www.rsc.org/

The first “half-sandwich” Yb^{III} single-ion magnets (SIMs) based on [12-MC_{Zn(II)}-4] are reported, in which the central ytterbium ion is coordinated by YbO₈ geometry in D_{4d} symmetry. The anisotropic barrier is extracted from the analysis of static, dynamic magnetism and emission spectrum offering an insight into the magneto-optical correlation.

Single molecule magnets (SMMs)¹ have received considerable attention for their intriguing magnetic behaviour and potential applications in high density data storage and quantum processing.² Towards this goal a challenge is of improvement for the reversal energy barrier (ΔE) and blocking temperature (T_B).³ In this regard, lanthanide ions look especially fascinating due to their large angular momentum and high spin-orbit coupling.⁴ Accordingly, Coronado and Torres et al. reported a double-deck phthalocyanine (H₂Pc) lanthanide-based single-ion magnet (SIM) [Tb(Pc)(Pc')]⁺, immensely increasing the energy barrier to a record value of 939 K.⁵ More research of the double-deck lanthanide complexes has elucidated the high ΔE and/or T_B are related to crystal field with highly axial symmetry.⁶ It has been established in lots of studies that energy barrier relies heavily on the significant anisotropy, which is strongly influenced by the ligand-field (LF).^{7,8} Therefore, how to create a compatible LF environment around lanthanide ion has been becoming an important task. Recently, Long and co-workers gave a prediction the single-ion anisotropy can be simply increased by prudently choosing the coordination environment around lanthanide ion.⁹

Moreover, to construct ideal LF environment we cannot ignore the importance of the control of the local symmetry for lanthanide ion.¹⁰ Herein, some significant examples can be referenced. The classical double-deck [Tb(Pc)₂]⁺ features D_{4d} symmetry concerning Tb^{III} ion sphere with the energy barrier of 374 K.⁶ The SIMs related to the organometallic sandwich,¹¹ for instance, [Er(COT)₂]⁺ (COT =

cyclooctatetraenide) with D_{8h} symmetry for centred Er^{III} ion has held the second largest T_B value of 10K.^{11d} Lately, our group reported a Schiff-base complex, [Fe₂Dy(L)₂(H₂O)]ClO₄·2H₂O, with a D_{5h} Dy^{III} ion bound to seven oxygen atoms. It recorded the highest ΔE of 459 K among d-f SIMs.^{10c} These cases featuring the high rotational symmetries are apt to achieve perceivable axial anisotropy and beneficial to suppress the quantum tunnelling of magnetization (QTM), thus resulting in the high energy barrier. Pursuing this clue, we focus on the creation of D_{4d} symmetry geometry, following a popular way to construct SIMs, including field-induced SIMs.

For D_{4d} symmetry, the [12-MC-4] ring (MC = metallacrown) with a 4-fold axis is thought for good candidate to create appropriate LF environment. MCs discovered by Pecoraro and Lah¹² are inorganic analogs of crown ethers and commonly formed with 3d metal ions featuring the -[M-X-Y-Z···]_n- motives (M = metal ion; X/Y/Z represent heteroatoms). As incorporation with diverse M^{II/III} ions (M = Mn, Fe, Co, Ni, Cu, Zn), the MCs configurations are various and can be assembled in fashion of [9-MC-3], [12-MC-4], [15-MC-5], [16-MC-5], etc. with combination of the alternating ligands.¹² Furthermore, the central cavities of some MCs also can be filled by lanthanide ions, leading to the SMMs/SIMs behaviours.¹³ To our knowledge, there is hardly report on the Yb^{III}-centred SIM based on [12-MC-4], except for the structures of the Ln[12-MC_{Zn(II)}-4]_n analogs (Ln = La, Nd, Tb, Dy, Er) disclosed lately.^{12d} Actually, a limited number of SMMs only Yb^{III}-containing have been reported to date.^{14,15}

With this in mind, we combined the [12-MC_{Zn(II)}-4] with Yb^{III} ion to construct SIMs involving in the near-infrared (NIR) emitting behaviour as well. The reaction between quinaldichydroxamic acid (Hquinha), Zn^{II} triflate, and Yb^{III} triflate in dimethylformamide (DMF) with the presence of trimethylamine was conducted. After addition of pyridine/isoquinoline (py/iqn) for crystallization, the subsequent mixture gave the ytterbium adduct respectively, formulated as [YbZn₄(quinha)₄(py)₄(DMF)₄](CF₃SO₃)₃·5DMF·7H₂O (**1**) and [YbZn₄(quinha)₄(iqn)₄(DMF)₄](CF₃SO₃)₃·6DMF·4H₂O (**2**). The phase purity was confirmed by X-ray powder diffraction studies (Figure S1).

The single X-ray crystallography data (Table S1) reveals **1** crystallizes in P4/ncc space group with the structure shown in Figures 1 and S2. Quinha serves as aditopic ligand and bridges Zn^{II}

MOE Key Lab of Bioinorganic and Synthetic Chemistry, School of Chemistry & Chemical Engineering, Sun Yat-Sen University, Guangzhou 510275, P. R. China. E-mail: jiajh3@mail.sysu.edu.cn; tongml@mail.sysu.edu.cn.

† Electronic Supplementary Information (ESI) available: experimental details, structural figures, crystallographic data (CCDC 1055953 and 1055954), magnetic and spectroscopic characterization. See DOI:10.1039/x0xx00000x

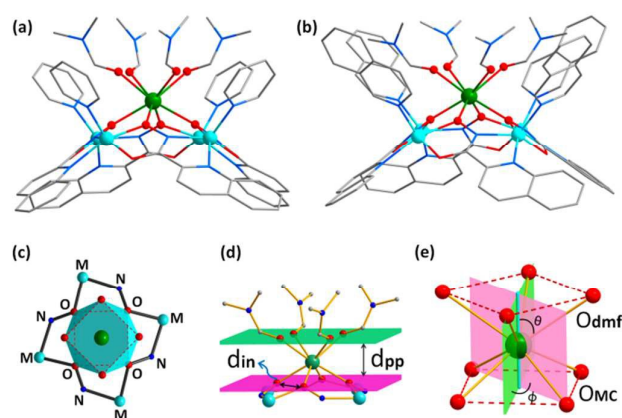


Figure 1. Side view of the structure of Yb[12-MC_{Zn(II)}-4] cation (**1**, *a*; **2**, *b*; Yb, olive; Zn, cyan; O, red; N, blue; C, gray). H atoms are omitted for clarity. Square-antiprismatic coordination of Yb[12-MC_{Zn(II)}-4] (*c*). Perspective showing d_{in} and d_{pp} (*d*), ϕ and ϑ (*e*) structural features, respectively.

ions forming a [12-MC_{Zn(II)}-4] ring with -[Zn-N-O]- as repeat unit. Each Zn^{II} ion is five-coordinated with one pyridine ligand bound axially. The central Yb^{III} ion is surrounded by the [12-MC_{Zn(II)}-4] ring and four DMF molecules. The bowl shape metallacrown presents four hydroximate oxygen atoms (O_{MC}) in a planar square, while the four oxygen atoms (O_{dmf}) of DMF molecules serve as another square. The two squares encapsulate the Yb^{III} ion forming a quasi-double-deck structure. The Continued Shape Measurements (CSHM) with SHAPE 2.0 software was performed to determine the LF symmetry of Yb^{III} ion, and the results are listed in Table S2. The smaller value means the closer coordination geometry to the ideal model. In addition, the skew angle (ϕ)¹⁶ defined as the offset between two squares is twisted 45.7° with respect to each other. In contrast to the ideal D_{4d} symmetry with $\phi = 45^\circ$, the minimum of the mean absolute deviation for ϕ (MAD $_{\phi}$) in Table S3 indicates the Yb^{III} coordination site can be described as a slightly distorted square antiprism. Per the data, **1** approximates theoretically to the ideal D_{4d} LF symmetry with a crystallographic 4-fold axis (Table S4).

Complex **2** is isostructural with **1** except for the isoquinoline molecules as axial ligands bound to Zn^{II} ions. Differing from **1**, however, **2** crystallizes in $P2_1/c$ space group without crystallographic centrosymmetry. The square antiprismatic coordination geometry is more distorted than that of **1**, with skew angle (ϕ) fluctuating wildly from 41.3° to 48.1°. The MAD $_{\phi}$ of 2.8(1)° (Table S3) lies in the medium level as the same order as the POM-based Er-SIMs (POM = polyoxometalates), but larger than that of **1**. Yb-O distances also support this major distortion. The Yb-O_{MC}/O_{dmf} bond lengths for **2** range from 2.279 to 2.322 Å and 2.391 to 2.424 Å, respectively, while these distances of **1** are clear 2.283 and 2.386 Å individually. The distance of Yb^{III} ion to [O_{MC}] plane is 0.245 Å shorter than that of Yb^{III} ion to [O_{dmf}] plane, since four DMF molecules of upper decker could swing in a disorder way. This differential becomes larger for **1** with value of 1.115 Å, mostly due to steric effect resulting from isoquinoline molecules. The ratio of d_{pp}/d_{in} was defined to clarify the extent of axial compression (or

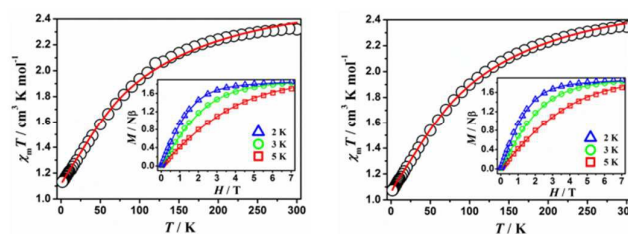


Figure 2. Temperature dependence of $\chi_m T$ product at 1000 Oe dc field of **1** (*left*) and **2** (*right*) with the solid lines for PHI fit (red). Inset: field dependence of the magnetization at 2.0, 3.0, and 5.0 K, respectively. The solid lines are for PHI fit (red, blue, and green).

elongation).¹⁶ In comparison with the selected compounds in Table S3, **2** has almost identical value with that in POM-based complexes ([Er(POM_a)₂]⁹ and [Er(POM_b)₂]¹³). It comes out that they all suffer a certain axial compression of the square antiprism formed by the eight-coordinated lanthanide ion. These differences would relate to the SMM behaviour based on the theory that prolate Yb^{III} ion can be stabilized with the appropriate LF environment.

The direct-current (dc) magnetic susceptibility measurements in Figure 2 show the values of $\chi_m T$ at room temperature are equal to 2.32 and 2.35 cm³·mol⁻¹ for **1** and **2**, respectively. Both are consistent with the expected value of 2.57 cm³·mol⁻¹ (Yb^{III}, ²F_{7/2}, $S = 1/2$, $L = 3$, $J = 7/2$, $g_J = 8/7$). Upon cooling, the $\chi_m T$ values gradually decrease to 1.13 cm³·mol⁻¹ (**1**) and 1.07 cm³·mol⁻¹ (**2**) at 1.8 K due to the thermal depopulation of the excited Stark sublevels resulting from the spin-orbit coupling and ligand-field effects of Yb^{III} ion. The field dependence of magnetization (Figure 2, inset) rises slowly at low temperature before reaching 1.85 N β (**1**) and 1.74 N β (**2**). The non-overlapping curves indicate the existence of magnetic anisotropy for two complexes. In search of quantitative information for energy-levels and the eigenstates, we have fitted the dc magnetic susceptibilities using the program PHI¹⁷ with the crystal-field perturbations. The Hamiltonian for the slightly distorted D_{4d} environment is proposed as:

$$\hat{H} = B_2^0 O_2^0 + B_4^0 O_4^0 + B_4^4 O_4^4 + B_6^0 O_6^0 + B_6^4 O_6^4$$

The best fit curves are presented in Figure 2. For both compounds the fits of the M - H curves at 2.0, 3.0, 5.0 K are reproduced well. The energy-levels and the eigenstates are listed in Table S5. The eigenstates for both compounds are impure, and the ground state doublets are mixed with $\pm 5/2$ and $\pm 3/2$ m_J states in ratio 78.9 : 21.1 % (**1**) and 93.4 : 6.6 % (**2**). This can be attributed to the reason that the [O_{MC}] square formed by four -O_{MC} is negative charged, comparing with the neutral [O_{dmf}] square, which may cause the presence of the transversal tensor, further making the m_J states mixed each other. For **1** the appropriate simulation of the ground state multiplet ²F_{7/2} is obtained with energy-level order of $m_J = \pm 5/2$ (0 cm⁻¹), $\pm 7/2$ (116 cm⁻¹), $\pm 3/2$ (468 cm⁻¹), $\pm 1/2$ (522 cm⁻¹), whereas for **2** the simulation gives different sequence of $m_J = \pm 5/2$ (0 cm⁻¹), $\pm 7/2$ (109 cm⁻¹), $\pm 1/2$ (505 cm⁻¹), $\pm 3/2$ (600 cm⁻¹). Thus the energy gaps of the first excited Kramers doublets are 116 cm⁻¹ (**1**) and 119 cm⁻¹ (**2**), respectively.

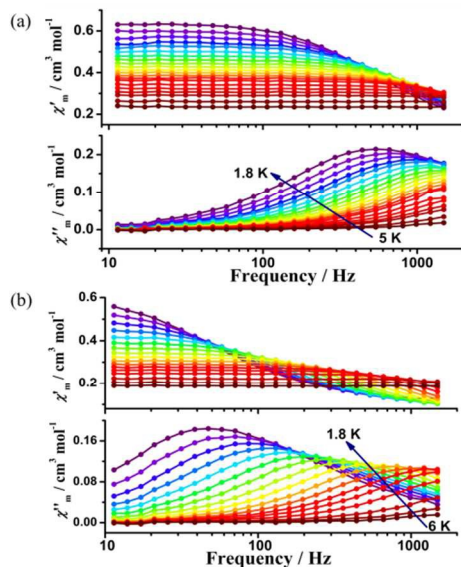


Figure 3. Frequency dependence of the in-phase and out-of-phase susceptibilities for **1**(a) and **2**(b) under a 600 Oe dc field.

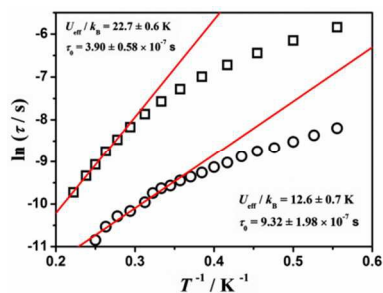


Figure 4. Temperature dependence of the relaxation time for **1** (circle) and **2** (square). The red solid line represents the Arrhenius law fit.

Alternating-current (ac) susceptibility measurements were performed to study the dynamic magnetic behavior. In the absence of dc field, no out-of-phase signal (χ'') was observed above 1.8 K due to the fast QTM effect. Generally, the QTM can be suppressed by the application of a small dc field. Thus by applying an optimized dc field of 600 Oe (Figure S4), the magnetic slow relaxation is observed (Figure 3). **1** and **2** are both considered as field-induced SIMs. So far as we know, it is the first report of the Yb^{III}-SIMs based on [12-MC-4] with D_{4d} symmetry geometry.

The relaxation time (τ) can be obtained from the fit of the frequency dependent ac susceptibility data with a generalized Debye function. In general, the τ is described as: $\tau^{-1} = AT + BT^n + C\exp(-\Delta/k_B T)$. The three terms represent the direct, Raman and Orbach relaxation process, respectively.¹⁸ In order to investigate the relaxation mechanism of the Yb^{III} ion, we plotted the relaxation time τ versus T on a log-log scale. The fitting curves in Figure S5 reveal τ are close to the T^n behavior. Further both

considering the direct and Raman process, the plot of τ versus T (Figure S5) gives the satisfied fitting results ($n = 5.7$), suggesting an

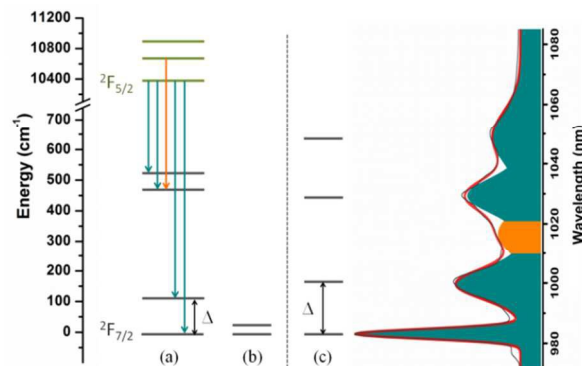


Figure 5. Energy levels of the ${}^2F_{7/2}$ ground state multiplet determined from the (a) dc fit ($\Delta = 116 \text{ cm}^{-1}$), (b) ac fit ($U_{\text{eff}}/k_B = 16 \text{ cm}^{-1}$), and (c) the luminescence spectrum ($\Delta = 169 \text{ cm}^{-1}$). Area of Gaussian deconvolution corresponding to the four Kramer doublets (dark cyan) and one hot transition (orange).

admixture of the direct and/or Raman process is dominant. The similar relaxation behaviour has been reported on a six-coordinated Yb^{III}-SIM.¹⁸ We tentatively try the Arrhenius law in the high temperature to evaluate the “effective energy barrier”, $U_{\text{eff}}/k_B = 12.6(7) \text{ K}$ (9 cm^{-1}), $\tau_0 = 9.32 \times 10^{-7} \text{ s}$ for **1** and $U_{\text{eff}}/k_B = 22.76(6) \text{ K}$ (16 cm^{-1}), $\tau_0 = 3.90 \times 10^{-7} \text{ s}$ for **2**. These values are several times smaller than energy gaps extracted from emission spectra of the excited Kramer doublets (109 cm^{-1} for **1**, 116 cm^{-1} for **2**; *vide infra*). Therefore, the thermally activated relaxation process (Orbach) can be excluded. Cole-Cole plots are quasi-semicircle with $\alpha = 0.01$ - 0.12 (**1**) and $\alpha = 0.04$ - 0.22 (**2**), indicating a narrow distribution of slow relaxation (Figure S6).

By incorporation of MCs, both **1** and **2** exhibit a set of NIR peaks from ca. 960 to 1080 nm when excited individually by 430 nm and 380 nm at room temperature (Figure S7). The radiative decay curves in Figure S8 reveal the lifetimes to be $3.6 \mu\text{s}$ for **1** and $3.1 \mu\text{s}$ for **2**, respectively. These are indicative that MCs have absorbed and transferred energy to lanthanide ion as a type of organometallic antenna. Furthermore, the study of the correlation between magnetic and luminescent properties bulks large among those compounds with emissions in the NIR region.¹⁵ In order to obtain the energy splitting of m_j states of the multiplet ground state, the structured spectroscopies were recorded at low temperature (Figure S9 and S10). Herein, **2** is taken for example. The emission profile (Figure 5) can be deconvoluted in four transitions ($10172, 10003, 9715, 9532 \text{ cm}^{-1}$) and one hot transition (9836 cm^{-1}). The former should be assigned to the ${}^2F_{5/2}$ to ${}^2F_{7/2}$ transitions, whereas the latter namely “hot band” can be attributed to thermally radiation from the higher crystal field sublevel of the ${}^2F_{5/2}$ state. The energy gap between the first excited and the ground states of the ${}^2F_{7/2}$ state is equal to 169 cm^{-1}

¹. This gap is close to the energy difference (116 cm⁻¹) obtained from the dc data fit, but evidently deviating from the energy barrier got from the ac analysis. In this respect, the effect of QTM cannot be neglected for the sake of SMMs with higher energy barrier.

In summary, we have reported two “half-sandwich” Yb^{III}-SMMs bearing MCs. The Yb^{III} ion in each Yb[12-MC_z(II)-4] compound has a square antiprismatic geometry with D_{4d} symmetry. The anisotropic barrier is extracted from the analysis of static, dynamic magnetism and emission spectrum offering an insight into the magneto-optical correlation. Further study would be focused on introduction of the compatible LF environment with axial compression to refresh the energy barrier for Yb^{III}-SMMs as well as the NIR property.

This work was supported by the “973 Project” (2014CB845602 and 2012CB821704), the NSFC (Grant nos 21301197, 91122032, 21371183 and 91422302) and the NSF of Guangdong (S2013020013002).

Notes and references

- R. Sessoli, D. Gatteschi, A. Caneschi and M. A. Novak, *Nature*, 1993, **365**, 141.
- D. Gatteschi, R. Sessoli and R. Villain, *Molecular Nanomagnets*, Oxford University Press: New York, 2006.
- (a) R. J. Blagg, L. Ungur, F. Tuna, J. Speak, P. Comar, D. Collison, W. Wernsdorfer, E. J. L. McInn, L. F. Chibotaru, R. E. P. Winpenny, *Nat. Chem.*, 2013, **5**, 673; (b) J. D. Rinehart, M. Fang, W. J. Evans and J. R. Long, *Nat. Chem.*, 2011, **3**, 538; (c) S.-D. Jiang, B.-W. Wang, G. Su, Z.-M. Wang, S. Gao, *Angew. Chem. Int. Ed.*, 2010, **49**, 7448; (d) Y.-N. Guo, G.-F. Xu, P. Gamez, L. Zhao, S.-Y. Lin, R. Deng, J. Tang and H.-J. Zhang, *J. Am. Chem. Soc.*, 2010, **132**, 8538.
- (a) L. Sorace, C. Benelli and D. Gatteschi, *Chem. Soc. Rev.*, 2011, **40**, 3092; (b) D. N. Woodruff, R. E. P. Winpenny and R. A. Layfield, *Chem. Rev.*, 2013, **113**, 5110; (c) F. Habib and M. Murugesu, *Chem. Soc. Rev.*, 2013, **42**, 3278.
- C. R. Ganivet, B. Ballesteros, G. de la Torre, J. M. Clemente-Juan, E. Coronado and T. Torres, *Chem. Eur. J.*, 2013, **19**, 1457.
- (a) N. Ishikawa, M. Sugita, T. Ishikawa, S. Koshihara and Y. Kaizu, *J. Am. Chem. Soc.*, 2003, **125**, 8694; (b) N. Ishikawa, M. Sugita, T. Ishikawa, S.-y. Koshihara and Y. Kaizu, *J. Phys. Chem. B*, 2004, **108**, 11265; (c) N. Ishikawa, M. Sugita and W. Wernsdorfer, *J. Am. Chem. Soc.*, 2005, **127**, 3650.
- (a) N. Ishikawa, M. Sugita, T. Okubo, N. Tanaka, T. Lino and Y. Kaizu, *Inorg. Chem.*, 2003, **42**, 2440; (b) C.-F. Wang, J.-L. Zuo, B. M. Bartlett, Y. Song, J. R. Long and X.-Z. You, *J. Am. Chem. Soc.*, 2006, **128**, 7162; (c) F. Neese and D. A. Pantazis, *Faraday Discuss.*, 2011, **148**, 229.
- (a) J.-L. Liu, F.-S. Guo, Z.-S. Meng, Y.-Z. Zheng, J.-D. Leng, M.-L. Tong, L. Ungur, L. F. Chibotaru, K. J. Heroux and D. N. Hendrickson, *Chem. Sci.*, 2011, **2**, 1268; (b) P. Zhang, L. Zhang, C. Wang, S. Xue, S.-Y. Lin and J. Tang, *J. Am. Chem. Soc.*, 2014, **136**, 4484; (c) D. Zeng, M. Ren, S.-S. Bao, L. Li and L.-M. Zheng, *Chem. Commun.*, 2014, **50**, 8356; (d) A. J. Brown, D. Pinkowicz, M. R. Saber and K. R. Dunbar, *Angew. Chem., Int. Ed.*, 2015, DOI:10.1002/anie.201411190.
- J. D. Rinehart and J. R. Long, *Chem. Sci.*, 2011, **2**, 2078.
- (a) J. J. Baldoví, J. J. Borrás-Almenar, J. M. Clemente-Juan, E. Coronado and A. Gaita-Ariño, *Dalton Trans.*, 2012, **41**, 13705; (b) J.-L. Liu, Y.-C. Chen, Y.-Z. Zheng, W.-Q. Lin, L. Ungur, W. Wernsdorfer, L. F. Chibotaru and M.-L. Tong, *Chem. Sci.*, 2013, **4**, 3310; (c) J.-L. Liu, J.-Y. Wu, Y.-C. Chen, V. Mereacre, A. K. Powell, L. Ungur, L. F. Chibotaru, X.-M. Chen, M.-L. Tong, *Angew. Chem. Int. Ed.*, 2014, **53**, 12966.
- (a) S. D. Jiang, B. W. Wang, H. L. Sun, Z. M. Wang and S. Gao, *J. Am. Chem. Soc.*, 2011, **133**, 4730; (b) M. Jeletic, P.-H. Lin, J. J. L. Roy, I. Korobkov, S. I. Gorelsky and M. Murugesu, *J. Am. Chem. Soc.*, 2011, **133**, 19286; (c) K. R. Meihaus and J. R. Long, *J. Am. Chem. Soc.*, 2013, **135**, 17952.
- (a) M. S. Lah and V. L. Pecoraro, *J. Am. Chem. Soc.*, 1989, **111**, 7258; (b) J. J. Bodwin, A. D. Cutland, R. G. Malkani and V. L. Pecoraro, *Coord. Chem. Rev.*, 2001, **216-217**, 489; (c) G. Mezei, C. M. Zaleski and V. L. Pecoraro, *Chem. Rev.*, 2007, **107**, 4933; (d) J. Jankolovits, J. W. Kampf and V. L. Pecoraro, *Inorg. Chem.*, 2014, **53**, 7534.
- (a) C. M. Zaleski, E. C. Depperman, J. W. Kampf, M. L. Kirk and V. L. Pecoraro, *Inorg. Chem.*, 2006, **45**, 10022; (b) H. L. C. Feltham, F. Klöwer, S. A. Cameron, D. S. Larsen, Y. Lan, M. Tropiano, S. Faulkner, A. K. Powell and S. Brooker, *Dalton Trans.*, 2011, **40**, 11425; (c) A. Yamashita, A. Watanabe, S. Akine, T. Nabeshima, M. Nakano, T. Yamamura and T. Kajiura, *Angew. Chem. Int. Ed.*, 2011, **50**, 4016; (d) F. Cao, S. Wang, D. Li, S. Zeng, M. Niu, Y. Song and J. Dou, *Inorg. Chem.*, 2013, **52**, 10747.
- (a) M.-E. Boulon, G. Cucinotta, J. Luzon, C. Degl’Innocenti, M. Perfetti, K. Bernot, G. Calvez, Z. Caneschi and R. Sessoli, *Angew. Chem. Int. Ed.*, 2013, **52**, 350; (b) H. L. C. Feltham, Y. Lan, F. Klöwer, L. Ungur, L. F. Chibotaru, A. K. Powell and S. Brooker, *Chem. Eur. J.*, 2011, **17**, 4362; (c) P.-H. Lin, W.-B. Sun, Y.-M. Tian, P.-F. Yan, L. Ungur, L. F. Chibotaru and M. Murugesu, *Dalton Trans.*, 2012, **41**, 12349; (d) Q. W. Li, J. L. Liu, J. H. Jia, J. D. Leng, W. Q. Lin, Y. C. Chen and M. L. Tong, *Dalton Trans.*, 2013, **42**, 11262; (e) T.-Q. Liu, P.-F. Yan, F. Luan, Y.-X. Li, J.-W. Sun, C. Chen, F. Yang, H. Chen, X.-Y. Zou and G.-M. Li, *Inorg. Chem.*, 2015, **54**, 221.
- (a) F. Pointillart, B. L. Guennic, S. Golhen, O. Cador, O. Maury and L. Ouahab, *Chem. Comm.*, 2013, **49**, 615; (b) F. Pointillart, B. L. Guennic, I. Cauchy, S. Golhen, O. Cador, O. Maury and L. Ouahab, *Inorg. Chem.*, 2013, **52**, 5978; (c) G. Cosquer, F. Pointillart, J. Jung, B. L. Guennic, S. Golhen, O. Cador, Y. Guyot, A. Brenier, O. Maury and L. Ouahab, *Eur. J. Inorg. Chem.*, 2014, **69**; (d) X. Yi, K. Bernot, V. L. Corre, G. Calvez, F. Pointillart, O. Cador, B. L. Guennic, J. Jung, O. Maury, V. Placide, Y. Guyot, T. Roisnel, C. Daiguebonne and O. Guillou, *Chem. Eur. J.*, 2014, **20**, 1569.
- (a) M. A. Aldamen, J. M. Clemente-Juan, E. Coronado, C. Martí-Gastaldo and A. Gaita-Ariño, *J. Am. Chem. Soc.*, 2008, **130**, 8874; (b) M. A. Aldamen, S. Cardona-Serra, J. M. Clemente-Juan, E. Coronado, A. Gaita-Ariño, C. Martí-Gastaldo, F. Luis and O. Montero, *Inorg. Chem.*, 2009, **48**, 3467.
- N. F. Chilton, R. P. Anderson, L. D. Turner, A. Soncini and K. S. Murray, *J. Comput. Chem.*, 2013, **34**, 1164.
- J. L. Liu, K. Yuan, J. D. Leng, L. Ungur, W. Wernsdorfer, F. S. Guo, L. F. Chibotaru and M. L. Tong, *Inorg. Chem.*, 2012, **51**, 8538.

Table of Content

Two examples of “half-sandwich” Yb^{III} single-ion magnets are presented bearing metallacrowns (MCs). The Yb^{III} ion in each Yb[12-MC_{Zn(II)}-4] compound has a square antiprismatic geometry with the D_{4d} symmetry. The anisotropic barrier is extracted from the analysis of static, dynamic magnetism and emission spectrum offering an insight into the magneto-optical correlation.

